# EFFECT OF DAMAGE ON THE TORSIONAL BUCKLING OF CARBON/EPOXY DRIVE SHAFTS WITH A SHELL THEORY

O. Montagnier[1,*] and Ch. Hochard[2]

[1] *Centre de recherche de l'Armée de l'air (CReA) - EOAA,*
*Base Aérienne 701, 13361 Salon Air, France*
[2] *Laboratoire de Mécanique et d'Acoustique (LMA),*
*31 chemin Joseph Aiguier, 13402 Marseille Cedex 20, France*
[*] *oliviermontagnier@inet.air.defense.gouv.fr*

**Keywords:** buckling ; shell theory ; torsion ; damage ; carbon/epoxy ; drive shaft.

**Abstract**

*This work is concerned with the effect of the damage on the torsional buckling of CFRP drive shafts. A buckling shell theory is developed to investigate this effect. This one is based on Flügge's shell theory, laminate theory and Flügge's solution for long tubes assumption. In a first step, the effect of damage on buckling torque is simply obtained by decreasing the transverse and shear modulus. Then, an iterative procedure including a damage model is considered to show the evolution of the buckling torque during the increase of static torque. The damage decreases the buckling load of all laminates studied but with various proportions.*

## 1 Introduction

Since the 1970s, composite materials have been regarded as potential candidates for manufacturing drive shafts of many kinds because of their high: specific stiffness and strength. Because these composite shafts are thin and subjected to torsion load, a risk of torsional buckling exists. This work is concerned with the effect of the carbon/epoxy damage on the torsional buckling load. In this case, the material damage (matrix micro-cracking, fibre/matrix debonding, transverse rupture) can have two origins. The first one is simply due to torsion load up to buckling (influence of prebuckling deformations and stresses). The second one is due to the rotation of the drive shaft. For example, when a shaft operate above the first critical speed, in the so-called supercritical regime, a repetitive bending appears at each acceleration and deceleration operations. The damage modify the modulus as the buckling load.

The finite element method is the most frequently employed method of computing torsional buckling. However, it is suitable a method requiring less computing time for the optimisation of carbon/epoxy drive shaft [1, 2]. Shell theory is used here. Laminate theory is included in Flügge's shell equations [3]. Assuming that we are dealing with a long cylinder, we can solve the shell equations with the simplified displacement field proposed by Flügge [3]. A simple way to model damage is to decrease the ply modulus concerned (transverse and shear). A conservative approach is obtain when the damage variables are taken to the minimum observed experimentally. A more complete approach is to consider an iterative procedure including a damage model [4]. Then it is possible to apply any path of load to create the damage before torsional buckling.

## 2 Composite damage modeling

The damage is only considered in the plane of the ply and expressed in terms of loss of stiffness

$$E_1 = E_1^0 (1 - d_1) \quad \text{with} \quad d_1 \in [0, 1] \tag{1}$$
$$E_2 = E_2^0 (1 - d_2) \quad \text{with} \quad d_2 \in [0, 1] \tag{2}$$
$$G_{12} = G_{12}^0 (1 - d_{12}) \quad \text{with} \quad d_{12} \in [0, 1] \tag{3}$$

where $d_1$, $d_2$ and $d_{12}$ are the damage in axial, in transverse and in shear directions, respectively. These damage variables are initialy null then $E_1^0$, $E_2^0$ and $G_{12}^0$ are initial stiffness in axial, in transverse and in shear directions, respectively.

Assuming that we are dealing with plane stresses and small perturbations assumptions, the local strain energy of each ply can be written in terms of stresses as follows [4]

$$\mathrm{E} = \frac{1}{2}\left( \frac{\langle \sigma_1 \rangle_+^2}{E_1^0 (1 - d_1)} + \frac{\langle \sigma_1 \rangle_-^2}{E_1^0} + \frac{\langle \sigma_2 \rangle_+^2}{E_2^0 (1 - d_2)} + \frac{\langle \sigma_2 \rangle_-^2}{E_2^0} - 2\frac{\nu_{12}^0}{E_1^0}\sigma_1\sigma_2 + \frac{\sigma_{12}^2}{G_{12}^0 (1 - d_{12})} \right) \tag{4}$$

where $\langle . \rangle_+$ and $\langle . \rangle_-$ stand for positive part and negative part. Noting that there is no damage during compressive steps. Thermodynamic forces associated to internal variables can be deduced from strain energy

$$Y_{d_j} = \frac{\partial \mathrm{E}}{\partial d_j} = \frac{\langle \sigma_j \rangle_+^2}{2E_j^0 (1 - d_j)^2} \quad j \in \{1, 2\} \tag{5}$$
$$Y_{d_{12}} = \frac{\partial \mathrm{E}}{\partial d_{12}} = \frac{\sigma_{12}^2}{2G_{12}^0 (1 - d_{12})^2} \tag{6}$$

The coupling mechanism between damage in transverse and shear direction is accounted for by an equivalent thermodynamic force

$$Y_{eq} = aY_{d_2}^m + bY_{d_{12}}^n \tag{7}$$

where $a$, $b$, $m$ and $n$ are material parameters.

The damage variables are defined relatively to the material behaviour. In the fiber direction, the brittle fracture is described with a threshold model

$$d_1 = 1 \quad \text{if} \quad Y_{d_1} > Y_{d_1}^{\max} \tag{8}$$

The damage in the transverse direction is based on a statistic law [5]

$$d_2 = \left\langle 1 - \mathrm{e}^{-(Y_{eq} - Y_0)} \right\rangle_+ \quad \text{with} \quad \dot{d}_2 \geq 0 \tag{9}$$

The damage mechanisms like matrix micro-cracking decrease the transverse and shear stiffness at the same time. Accordingly, the damage in shear direction is assumed to be proportional to the previous one

$$d_{12} = cd_2 \tag{10}$$

## 3 Torsional buckling analysis

The finite element method is the most frequently employed method of computing torsional buckling. However, it is suitable here a method requiring less computing time. The other pos-

sibility consists in solving the buckling shell theory in the case of orthotropic circular cylinders. Flügge's buckling shell theory for cylinder is used here [3]. Equilibrium equations can be written in the following form

$$\begin{aligned} N_{x,x} + N_{yx,x} - 2Tu_{,xy} &= 0 \\ N_{y,y} + N_{xy,y} + \frac{1}{r}\left(M_{xy} + M_y\right)_{,y} - 2T\left(v_{,xy} + \frac{w_{,x}}{r}\right) &= 0 \\ M_{x,xx} + \left(M_{yx} + M_{xy}\right)_{,xy} + M_{y,yy} - \frac{N_y}{r} + 2T\left(\frac{v_{,x}}{r} + w_{,xy}\right) &= 0 \end{aligned}$$

where $N_x$ and $N_y$ are normal forces per unit thickness, $N_{xy}$ and $N_{yx}$ are shear forces per unit thickness, $T$ is the torque, $r$ is the medium radius and $(u, v, w)$ is the middle-surface cylinder displacement field.

The laminate theory is included in the shell equations as it can be seen in [6]. It gives the equilibrium equations of the torsional buckling problem for a circular cylinder with orthotropic properties

$$\begin{aligned} &\left(A_{11} + \frac{B_{11}}{r}\right)u'' + \left(2A_{13} - \frac{T}{\pi r^2}\right)\dot{u}' + \left(A_{33} - \frac{B_{33}}{r} + \frac{D_{33}}{r^2}\right)\ddot{u} \\ &+ \left(A_{13} + \frac{2B_{13}}{r} + \frac{D_{13}}{r^2}\right)v'' + \left(A_{12} + \frac{B_{12}}{r} + A_{33} + \frac{B_{33}}{r}\right)\dot{v}' \\ &+ A_{23}\ddot{v} - \left(\frac{B_{11}}{r} + \frac{D_{11}}{r^2}\right)w''' + A_{12}w' + \left(-\frac{B_{23}}{r} + \frac{D_{23}}{r^2}\right)\ddot{w} \\ &+ \left(A_{23} - \frac{B_{23}}{r} + \frac{D_{23}}{r^2}\right)\dot{w} + \left(-\frac{B_{12}}{r} - \frac{2B_{33}}{r} + \frac{D_{33}}{r^2}\right)\ddot{w}' - \left(\frac{3B_{13}}{r} + \frac{D_{13}}{r^2}\right)\dot{w}'' = 0 \end{aligned} \quad (11)$$

$$\begin{aligned} &\left(A_{13} + \frac{2B_{13}}{r} + \frac{D_{13}}{r^2}\right)u'' + \left(A_{12} + \frac{B_{12}}{r} + A_{33} + \frac{B_{33}}{r} - \frac{D_{33}}{2r^2}\right)\dot{u}' \\ &+ \left(A_{23} + \frac{3D_{23}}{2r^2}\right)\ddot{u} + \left(A_{33} + \frac{3B_{33}}{r} + \frac{5D_{33}}{2r^2}\right)v'' \\ &+ \left(2A_{23} + \frac{4B_{23}}{r} + \frac{2D_{23}}{r^2} - \frac{T}{\pi r^2}\right)\dot{v}' + \left(A_{22} + \frac{B_{22}}{r}\right)\ddot{v} \\ &- \left(\frac{B_{13}}{r} + \frac{2D_{13}}{r^2}\right)w''' + \left(A_{23} + \frac{B_{23}}{r} - \frac{T}{\pi r^2}\right)w' - \frac{B_{22}}{r}\ddot{w} \\ &+ A_{22}\dot{w} + \left(-\frac{B_{12}}{r} - \frac{D_{12}}{r^2} - \frac{2B_{33}}{r} - \frac{3D_{33}}{r^2}\right)\dot{w}'' + \left(-\frac{3B_{23}}{r} + \frac{D_{23}}{r^2}\right)\ddot{w}' = 0 \end{aligned} \quad (12)$$

$$\begin{aligned} &\left(\frac{B_{11}}{r} + \frac{D_{11}}{r^2}\right)u''' + \left(3\frac{B_{13}}{r} + \frac{D_{13}}{r^2}\right)\dot{u}'' + \left(2\frac{B_{33}}{r} - \frac{D_{33}}{r^2} + \frac{B_{12}}{r}\right)\ddot{u}' \\ &+ \left(\frac{B_{23}}{r} - \frac{D_{23}}{r^2}\right)\dddot{u} + \left(-A_{23} + \frac{B_{23}}{r} - \frac{D_{23}}{r}\right)\dot{u} + \left(\frac{B_{13}}{r} + \frac{2D_{13}}{r^2}\right)v''' \\ &+ \left(2\frac{B_{33}}{r} + \frac{3D_{33}}{r^2} + \frac{B_{12}}{r} + \frac{D_{12}}{r^2}\right)\dot{v}'' - A_{12}u' + \left(3\frac{B_{23}}{r} + \frac{2D_{23}}{r^2}\right)\ddot{v}' \\ &+ \frac{B_{22}}{r}\dddot{v} + \left(-A_{23} - \frac{B_{23}}{r} + \frac{T}{\pi r^2}\right)v' - A_{22}\dot{v} - \frac{D_{11}}{r^2}w'''' \\ &- \frac{4D_{13}}{r^2}\dot{w}''' - \left(\frac{4D_{33}}{r^2} + 2\frac{D_{12}}{r^2}\right)\ddot{w}'' - \frac{4D_{23}}{r^2}\dddot{w}' - \frac{D_{22}}{r^2}\ddddot{w} + \frac{3B_{12}}{r}w'' \end{aligned}$$

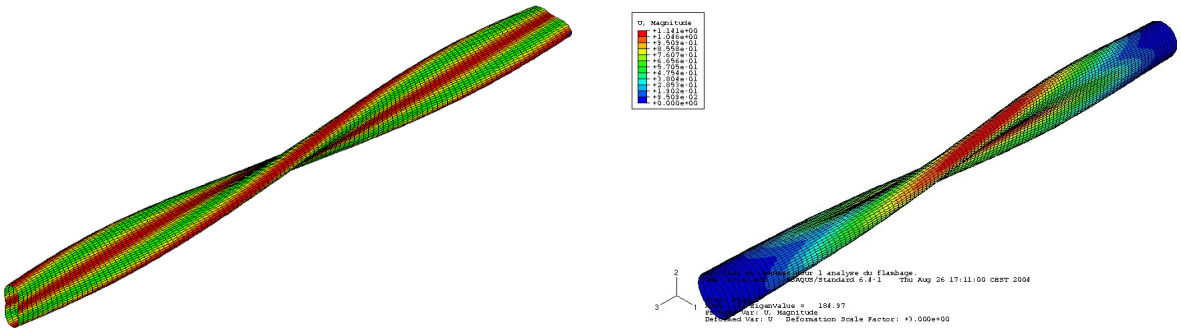

(a) Flügge's displacement field for torsional buckling of long cylinder (first mode)

(b) First mode of torsional buckling of a composite tube in ABAQUS

Figure 1: Graphical representations of torsional buckling

$$+\left(\frac{4B_{23}}{r}-\frac{2D_{23}}{r^2}-\frac{T}{\pi r^2}\right)\dot{w}'+\left(\frac{2B_{22}}{r}-\frac{2D_{22}}{r^2}\right)\ddot{w}+\left(-A_{22}+\frac{B_{22}}{r}-\frac{D_{22}}{r^2}\right)w \quad = \quad 0 \quad (13)$$

with $\_' = r\partial\_/\partial x$ , $\dot{\_} = \partial\_/\partial\varphi$ and where $\mathbf{A}$, $\mathbf{B}$ and $\mathbf{D}$ are the classical stiffness matrix of the laminate.

Because we are dealing with very long shaft, it is possible to neglect the boundary condition effects. In this case, a simplified displacement field proposed by Flügge can be used

$$u = a\sin(h\varphi+\frac{p\pi x}{l}), \quad v = b\sin(h\varphi+\frac{p\pi x}{l}), \quad w = c\cos(h\varphi+\frac{p\pi x}{l}) \qquad (14)$$

where $h$ is the number of half-wave along the cylinder circumference and $p$ is the number of half-wave along the cylinder axis of fictive length $l$. The first mode is represented in the Fig. 1a.

When this displacement field is applied to the shell equations, a classical eigenvalue problem is obtained

$$\mathbf{K}.\mathbf{U} = \mathbf{0} \quad \text{with} \quad \mathbf{U} = \begin{bmatrix} a \\ b \\ c \end{bmatrix} \qquad (15)$$

where $\mathbf{K}$ is the stiffness matrix

$$K(1,1) = -\left(A_{11}+\frac{B_{11}}{r}\right)\lambda^2-\left(2A_{13}-\frac{T}{\pi r^2}\right)h\lambda-\left(A_{33}-\frac{B_{33}}{r}+\frac{D_{33}}{r^2}\right)h^2 \qquad (16)$$

$$K(1,2) = -\left(A_{13}+\frac{2B_{13}}{r}+\frac{D_{13}}{r^2}\right)\lambda^2-\left(A_{12}+\frac{B_{12}}{r}+A_{33}+\frac{B_{33}}{r}\right)h\lambda-A_{23}h^2 \qquad (17)$$

$$K(1,3) = -\left(\frac{B_{11}}{r}+\frac{D_{11}}{r^2}\right)\lambda^3+A_{12}\lambda+\left(-\frac{B_{23}}{r}+\frac{D_{23}}{r^2}\right)h^3+\left(A_{23}-\frac{B_{23}}{r}+\frac{D_{23}}{r^2}\right)h$$
$$+\left(-\frac{B_{12}}{r}-\frac{2B_{33}}{r}+\frac{D_{33}}{r^2}\right)h^2\lambda-\left(\frac{3B_{13}}{r}+\frac{D_{13}}{r^2}\right)h\lambda^2 \qquad (18)$$

$$K(2,1) = -\left(A_{13}+\frac{2B_{13}}{r}+\frac{D_{13}}{r^2}\right)\lambda^2-\left(A_{12}+\frac{B_{12}}{r}+A_{33}+\frac{B_{33}}{r}-\frac{D_{33}}{2r^2}\right)h\lambda$$
$$-\left(A_{23}+\frac{3D_{23}}{2r^2}\right)h^2 \qquad (19)$$

$$K(2,2) = -\left(A_{33}+\frac{3B_{33}}{r}+\frac{5D_{33}}{2r^2}\right)\lambda^2-\left(2A_{23}+\frac{4B_{23}}{r}+\frac{2D_{23}}{r^2}-\frac{T}{\pi r^2}\right)h\lambda$$

$$- \left( A_{22} + \frac{B_{22}}{r} \right) h^2 \tag{20}$$

$$K(2,3) = - \left( \frac{B_{13}}{r} - \frac{2D_{13}}{r^2} \right) \lambda^3 + \left( A_{23} + \frac{B_{23}}{r} - \frac{T}{\pi r^2} \right) \lambda - \frac{B_{22}}{r} h^3 + A_{22} h \tag{21}$$

$$- \left( \frac{B_{12}}{r} + \frac{D_{12}}{r^2} + \frac{2B_{33}}{r} + \frac{3D_{33}}{r^2} \right) h\lambda^2 + \left( -\frac{3B_{23}}{r} + \frac{D_{23}}{r^2} \right) h^2 \lambda \tag{22}$$

$$K(3,1) = - \left( \frac{B_{11}}{r} + \frac{D_{11}}{r^2} \right) \lambda^3 - \left( 3\frac{B_{13}}{r} + \frac{D_{13}}{r^2} \right) h\lambda^2 - \left( 2\frac{B_{33}}{r} - \frac{D_{33}}{r^2} + \frac{B_{12}}{r} h^2 \right) \lambda$$
$$- \left( \frac{B_{23}}{r} - \frac{D_{23}}{r^2} \right) h^3 - A_{12}\lambda + \left( -A_{23} + \frac{B_{23}}{r} - \frac{D_{23}}{r} \right) h \tag{23}$$

$$K(3,2) = - \left( \frac{B_{13}}{r} + \frac{2D_{13}}{r^2} \right) \lambda^3 - \left( 2\frac{B_{33}}{r} + \frac{3D_{33}}{r^2} + \frac{B_{12}}{r} + \frac{D_{12}}{r^2} \right) h\lambda^2$$
$$- \left( 3\frac{B_{23}}{r} + \frac{2D_{23}}{r^2} \right) h^2 \lambda - \frac{B_{22}}{r} h^3 + \left( -A_{23} - \frac{B_{23}}{r} + \frac{T}{\pi r^2} \right) \lambda - A_{22} h \tag{24}$$

$$K(3,3) = -\frac{D_{11}}{r^2}\lambda^4 - \frac{4D_{13}}{r^2} h\lambda^3 - \left( \frac{4D_{33}}{r^2} + 2\frac{D_{12}}{r^2} \right) h^2\lambda^2 - \frac{4D_{23}}{r^2} h^3\lambda - \frac{D_{22}}{r^2} h^4$$
$$-\frac{3B_{12}}{r}\lambda^2 - \left( \frac{4B_{23}}{r} - \frac{2D_{23}}{r^2} - \frac{T}{\pi r^2} \right) h\lambda \tag{25}$$

$$- \left( \frac{2B_{22}}{r} - \frac{2D_{22}}{r^2} \right) h^2 + \left( -A_{22} + \frac{B_{22}}{r} - \frac{D_{22}}{r^2} \right) \tag{26}$$

with $\lambda = p\pi r/l$. A non-trivial solution exists when the determinant of $\mathbf{K}$ is null.

An efficient numerical method is implemented to reduce the computing time in the GA of [2]. The method consist in finding the minimun value of $T_{\text{buck}}$ that cancel the determinant of $\mathbf{K}$. The determinant depends also on two other unknowns which are $h \in \mathbb{N}^*$and $p \in \mathbb{R}^{*+}$. Numerically, it is observed that the minimum value of buckling torque is always obtain for $h = 2$. A time-expensive method consist in searching the values of $T_{\text{buck}}$ which cancel the determinant for all values of $p$ and then to find the minimum of $T_{\text{buck}}$. A less expensive approach is to consider the value of $p = l\left(48e^2/12r^2\right)^{1/4}/\pi r$ obtained by Flügge for the isotropic material case but this method can lead to large errors in some cases. Nevertheless, the exact value of $p$ can be search around the above value. Because we have observed that the determinant can be assumed linear in $T$ around $T_{\text{buck}}$, only some computations are necessary if we previously estimate the value of $T_{\text{buck}}$ with an analytic criterion like the Hayashi's criterion

$$T_{\text{buck}} = 11\sqrt{r} \left( A_{11} - \frac{A_{12}^2}{A_{22}} \right)^{1/4} D_{22}^{3/4} \tag{27}$$

It should be noted that this criterion like other classical criteria do not account for the coupling mechanism involved in unsymmetrical laminates.

## 4 Results

### *4.1 Buckling with initialy damaged tubes*

The shell method is tested on unsymmetrical stacking sequences in Table 1 and compared to the finite element method in case without damage effects. In the table, all the tubes have the same size and the laminate all have the same thickness. The results obtained with the finite element method using ABAQUS (s4 elements) [7], which were previously validated in [8] based on experimental results obtained by [9], are taken as reference values. An example of a buckling mode is given in the Figure 1b to show the effect of boudary conditions. The results obtained with shell theory show good agreement with finite element calculation giving a conservative

Table 1: Buckling torque of carbon/epoxy laminate tubes: comparison between methods of computation and effect of damage ($l = 4$ m, $r_{\mathrm{m}} = 40$ mm, $E_{11} = 134$ GPa, $E_{22} = 8.5$ GPa, $E_{66} = E_{55} = 4.6$GPa, $E_{44} = 4.0$ GPa, $E_{12} = 0.29$, $e_{\mathrm{s}} = 1.067$ mm)

| Laminate | | ABAQUS | | Flügge with laminate theory | | | | | |
|---|---|---|---|---|---|---|---|---|---|
| $d_2 = d_{12} =$ | | 0 | | 0 | | 0.5 | | 0.8 | |
| N° | | Mesh[a] | Nm | Nm | error % | Nm | % | Nm | % |
| 1 | $[15,-15]_4$ | 60-150 | 210 | 193 | -8 | 117 | -39 | 64 | -67 |
| 2 | $[30,-30]_4$ | 60-150 | 263 | 254 | -4 | 185 | -27 | 135 | -47 |
| 3 | $[45,-45]_4$ | 60-150 | 385 | 383 | -1 | 311 | -19 | 251 | -34 |
| 4 | $[0_2,45,-45,45,-45,0_2]$ | 60-150 | 230 | 218 | -5 | 155 | -29 | 114 | -48 |
| 5 | $[0_2,45,0,-45,0,45,-45]$ | 30-100 | 358 | 342 | -4 | 277 | -19 | 232 | -32 |
| 6 | [45,15,-15,-45,-15,15,45,-45] | 60-150 | 439 | 449 | 2 | 393 | -12 | 358 | -20 |

[a] Number of circumferential elements - number of lengthwise elements.

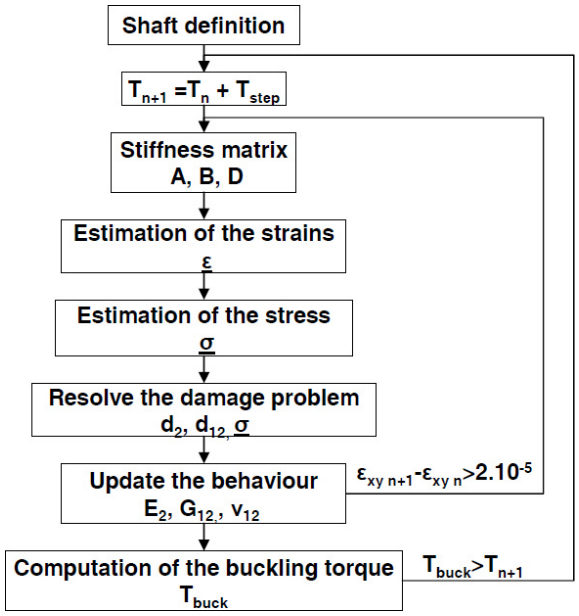


Figure 2: Algorithm to compute torsional buckling with damage effect

estimate on the whole. The largest errors amount to only 8% and the mean error is 4%. Note that it is shown in [8] that the long tube assumption investigated here, is useful when the length-to-diameter ratio is greater than 100 and the diameter-to-thickness ratio is greater than 40.

The buckling load is then computed on previously damaged tubes. This damage can be due, for example, to repetitive flexural oscillations. The damages variables $d_2$ and $d_{12}$ are assumed to be equal to 0.5 and 0.2, successively (Tab. 1). Comparatively to the case of a tube without damage, the buckling torque can be highly reduced. This load is divide by three in the case of a $[15, -15]_4$ laminate with 80% of damage in transverse and in shear directions. The influence is only of 20% in the case N°6.

*4.2 Buckling with initialy undamaged tubes*

In this case, the damage model is added to the buckling torque computation. The principle is represented in the Figure2. The algorithm is implemented in Matlab [10]. In particular, the non-linear damage problem is solved with a medium-scale algorithm of "fsolve". The influence of damage is shown on a $[0_2, 90_2]_s$ shaft (Fig. 3). Here the buckling torque is decreased by a value of 19%.

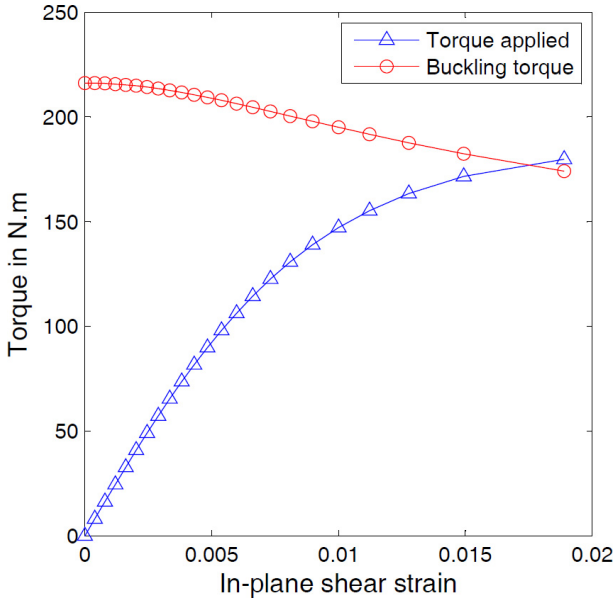


Figure 3: Evolution of buckling torque with the increase of static torque on a $[0_2, 90_2]_s$ shaft ($r_{\mathrm{m}} = 26$ mm, $E_{11} = 116.4$ GPa, $E_{22} = 9.5$ GPa, $E_{66} = 5.0$GPa, $E_{12} = 0.31$, $e_{\mathrm{s}} = 1$ mm, $a = 1$, $b = 1.85$, $c = 1$, $m = 1$, $n = 1$ and $Y_0 = 0$)

## 5 Conclusion

The results obtained with Flügge's theory on long tubes with laminate theory show good agreement with finite element calculation giving a conservative estimate on the whole. The method with the damage is then applied on several classical laminates. The damage decreases the buckling load of all laminates studied. The results show that damage effect on the buckling torque cannot be ignore if the drive-shaft is subject to bending fatigue. The damage effect is more significant for laminates including 0° and 90° plies.

## References

[1] O. Montagnier, C. Hochard, Optimization of supercritical carbon/epoxy drive shafts using a genetic algorithm, in: Proceedings of the 13th European Conference on Composite Materials, Stockholm, Sweden, 2008.

[2] O. Montagnier, C. Hochard, Optimisation of a high speed rotating composite drive shaft using a genetic algorithm-hybrid high modulus-high resistance carbon solutions, Arxiv preprint arXiv:1110.1628.

[3] W. Flügge, Stresses in shells, 2nd Edition, Springer-Verlag, Berlin, 1973.

[4] P. Ladevèze, E. Le Dantec, Damage modelling of the elementary ply for laminated composites, Composites Science and Technology 43 (3) (1992) 257–267.

[5] C. Hochard, S. Miot, N. Lahellec, F. Mazerolle, M. Herman, J. Charles, Behaviour up to rupture of woven ply laminate structures under static loading conditions, Composites Part A 40 (8) (2009) 1017–1023.

[6] C. Bert, C.-D. Kim, Analysis of buckling of hollow laminated composite drive shaft, Composites Science and Technology 53 (1995) 343–351.

[7] K. Hibbitt, I. Sorensen, ABAQUS/Standard: User's Manual, Hibbitt, Karlsson & Sorensen, 2001.

[8] O. Montagnier, Tubes composites à grande vitesse de rotation : analyses expérimentales et modélisation, Ph.D. thesis, University of Marseille, France (2005).

[9] O. A. Bauchau, T. M. Krafchack, J. F. Hayes, Torsional buckling analysis and damage tolerance of graphite/epoxy shafts, Journal of Composite Materials 22 (1988) 258–270.

[10] The MathWorks, MATLAB, The MathWorks Inc., http://www.mathworks.com, 1990.